

Evidence for the Blue 10π S_6^{2+} Dication in Solutions of $S_8(AsF_6)_2$:
A Computational Study Including Solvation EnergiesIngo Crossing^{*,†,‡} and Jack Passmore^{*,§}*Institut für Anorganische Chemie, Universität Karlsruhe, Engesserstr. Geb. 30.45,
76128 Karlsruhe, Germany, and Chemistry Department, University of New Brunswick,
Fredericton, New Brunswick, E3B 6E2 Canada*

Received December 30, 2002

The energetics of dissociation reactions of S_8^{2+} into stoichiometric mixtures of S_n^+ , $n = 2-7$, and S_m^{2+} , $m = 3, 4, 6, 10$, were investigated by the B3PW91 method [6-311+G(3df)//6-311+G*] in the gas phase and in solution, with solvation energies calculated using the SCIPCM model and in some cases also the COSMO model [B3PW91/6-311+G*, dielectric constants 2–30, 83, 110]. UV–vis spectra of all species were calculated at the CIS/6-311G(2df) level and for S_4^{2+} and S_6^{2+} also at the TD-DFT level (BP86/SV(P)). Standard enthalpies of formation at 298 K were derived for S_3^{2+} (2538 kJ/mol), S_6^{2+} (2238 kJ/mol), and S_{10}^{2+} (2146 kJ/mol). A comparison of the observed and calculated UV–vis spectra based on our calculated thermochemical data in solution suggests that, in the absence of traces of facilitating agent (such as dibromine Br_2), S_8^{2+} dissociates in dilute SO_2 solution giving an equilibrium mixture of ca. $0.5S_6^{2+}$ and S_5^+ ($K \approx 8.0$) while in the more polar HSO_3F some S_8^{2+} remains ($K \approx 0.4$). According to our calculations, the blue color of this solution is likely due to the $\pi^*-\pi^*$ transition of the previously unknown 10π S_6^{2+} dication, and the previously assigned S_5^+ is a less important contributor. Although not strictly planar, S_6^{2+} may be viewed as a 10π electron Hückel-aromatic ring containing a thermodynamically stable $3p_\pi-3p_\pi$ bond [$d(S-S) = 2.028$ Å; $\tau(S-S-S) = 47.6^\circ$]. The computations imply that the new radical cation S_4^+ may be present in sulfur dioxide solutions given on reaction of sulfur oxidized by AsF_5 in the presence of a facilitating agent. The standard enthalpy of formation of $S_6(AsF_6)_2(s)$ was estimated as -3103 kJ/mol, and the disproportionation enthalpy of $2S_6(AsF_6)_2(s)$ to $S_8(AsF_6)_2(s)$ and $S_4(AsF_6)_2(s)$ as exothermic by $6-17$ kJ/mol. The final preference of the observed disproportionation products is due to the inclusion of solvent molecules, e.g., AsF_3 , that additionally favors the disproportionation of $2S_6(AsF_6)_2(s)$ into $S_8(AsF_6)_2(s)$ and $S_4(AsF_6)_2(AsF_3)(s)$ by 144 kJ/mol.

Introduction

In 1804, Buchholz reported¹ that elemental sulfur dissolved in oleum (oxidizing agent: SO_3 added to 100% H_2SO_4 , reduced product SO_2) to give brown, green, and blue solutions depending on the SO_3 concentration. The species responsible for these colors have been the subject of numerous investigations.^{2–10} In 1969, the extremely blue

solid crystalline $S_8(AsF_6)_2$ was prepared^{11a} and its X-ray structure shown^{11c} to contain discrete S_8^{2+} dications. In solution, S_8^{2+} was in equilibrium with a radical cation, suggested^{11b} to be S_4^+ , as given in eq 1.



However, later the radical cation was unambiguously established¹² as S_5^+ by esr studies using 91.8% ^{33}S in oleum

* Correspondence regarding computational methods should be addressed to I.K., and correspondence regarding problem conception, development, and chemistry should be addressed to J.P. E-mail: crossing@chemie.uni-karlsruhe.de (I.K.); passmore@unb.ca (J.P.).

† Part of this work has been presented at the 14th American Chemical Society Winter Fluorine Chemistry Conference in St. Petersburg, FL, in January, 1999.

‡ Universität Karlsruhe.

§ University of New Brunswick.

(1) Bucholz, C. F. *Gehlen's Neues J. Chem.* **1804**, 3, 7.

(2) (a) Weber, R. J. *Prakt. Chem.* **1882**, 133, 218. (b) Masson, I.; Argument, C. J. *Chem. Soc.* **1938**, 1705.

(3) *Inorganic Sulphur Chemistry*; Nickless, G. Ed.; Elsevier: London, 1968; p 412.

(4) Auerbach, R. Z. *Phys. Chem. (Leipzig)* **1926**, 121, 337.

(5) McNeil, D. A. C.; Murray, M.; Symons, M. C. R. *J. Chem. Soc. A* **1967**, 1019.

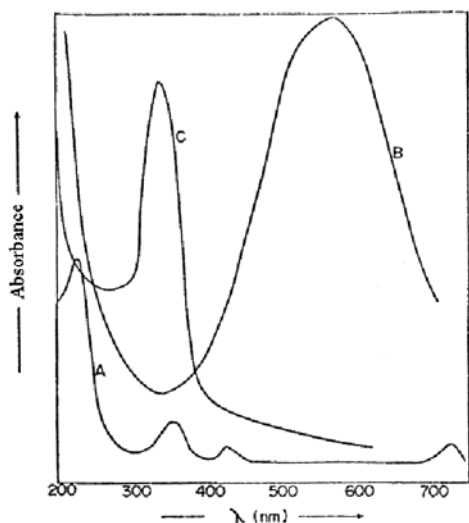


Figure 1. Experimental^{11b} UV-vis spectra of sulfur cations dissolved in HSO_3F . A denotes the " S_{16}^{2+} ", B the " S_8^{2+} ", and C the " S_4^{2+} " formal oxidation stage.

solutions. The S_8^{2+} was therefore in equilibrium with S_5^+ , as well as another unknown sulfur cation as shown in eq 2.



The blue color has been assigned to both S_8^{2+} ^{11a} and S_5^+ .^{7,12} However, the preparation of a sample of crystalline $S_8(AsF_6)_2$ ²² that was red in transmitted light showed that the blue color was not due to S_8^{2+} . Solid $S_8(AsF_6)_2$ dissolves in HSO_3F to give an intensely blue solution with a broad peak centered at 585 nm (UV-vis spectrum shown in Figure 1).^{11a,b} The more complex UV-vis spectra obtained in sulfur dioxide solution are shown in Figure 2.

The ESR spectra of S_8^{2+} in both HSO_3F and SO_2 showed the presence of S_5^+ and an additional radical that has been attributed to S_7^+ .^{7,13} This may be accounted for by eq 3:^{14,15}

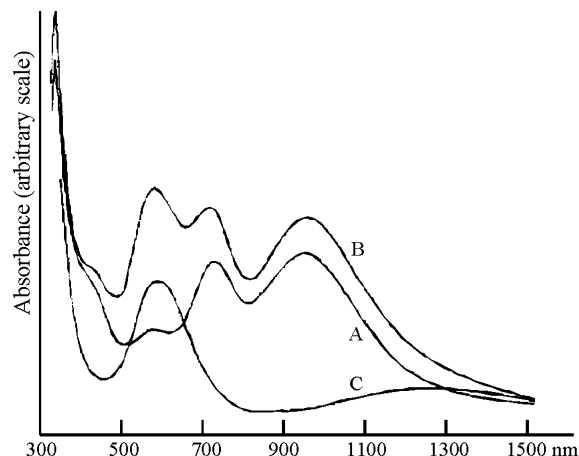
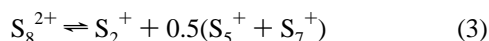
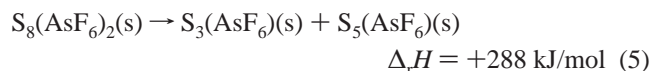
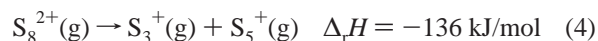


Figure 2. Experimental⁷ UV-vis spectra of the successive oxidation of elemental sulfur by AsF_5 in SO_2 solution. A denotes the " S_{16}^{2+} ", B the " S_8^{2+} ", and C the " S_4^{2+} " formal oxidation stage.

However, sulfur is oxidized by AsF_5 in the absence of a trace of facilitating agent¹⁶ (e.g., Br_2)^{7,17} only to S_8^{2+} , and not to S_4^{2+} ($2 \times S_2^+$).^{11ab,14,18–21} ESR studies showed that S_5^+ is not further oxidized by AsF_5 in SO_2 solution, even in large excess (in the absence of a facilitating agent). Therefore, equilibrium 3 is highly unlikely. In 1994, we determined¹⁴ the standard heat of formation of $S_8(AsF_6)_2(s)$. In 2000, we established^{22,23} that in the gas-phase S_8^{2+} was thermochemically unstable relative to various monocations including $2S_4^+$ (eq 1) and S_5^+ and S_3^+ (eq 2 with $? = S_3^+$). Therefore, in the solid state $S_8(AsF_6)_2$ is more stable than the monocation salts.^{21–23} For example,²² although in the gas phase a dissociation of S_8^{2+} to $S_3^+(g)$ and $S_5^+(g)$ is favorable by -136 kJ/mol (eq 4), solid $S_8(AsF_6)_2(s)$ is stable relative to $S_3(AsF_6)(s)$ and $S_5(AsF_6)(s)$ by 288 kJ/mol (eq 5):

- (15) (a) The standard heat of formation of $S_8As_6(s)$ was obtained¹⁴ by fluorine bomb calorimetry. The values of the enthalpies of dissociation of the gas phase of S_8^{2+} to sulfur monocations obtained in ref 14 used the results of a calculation of the combined first and second ionization potential of S_8 by ab initio calculations at the HF/3-21G* and HF/6-31G* level of theory. However, the calculated geometries were very different from the experimentally observed solid state structure of the S_8^{2+} dication found in different salts (see refs 11c and 22), especially the long transannular S–S bond. (b) $\Delta H_f(S_8^{2+}, g) = 2301$ kJ/mol. Grein, F.; Sannigrahi, M. University of New Brunswick, unpublished results at the HF/3-21G* and HF/6-31G* level of theory. However, later it was shown that this calculated enthalpy of formation of $S_8^{2+}(g)$ is substantially in error by 150 kJ/mol (see ref 22).
- (16) A facilitating agent reduces the activation energy of a reaction but, unlike a catalyst, is not recovered after the reaction occurred.
- (17) Mailman, A.; Passmore, J.; Wood, D. Work in progress.
- (18) (a) Passmore, J.; Sutherland, G. W.; White, P. S. *J. Chem. Soc., Chem. Commun.* **1980**, 330. (b) Passmore, J.; Sutherland, G. W.; White, P. S. *Inorg. Chem.* **1982**, 21, 2717. (c) Passmore, J.; Sutherland, G. W.; Widden, T. K.; White, P. S.; Wong, C. H. *Can. J. Chem.* **1985**, 63, 1209. (d) Dionne, I. M. Sc. Thesis, University of New Brunswick, 1993. (e) Faggiani, R.; Gillespie, R. J.; Sawyer, J. F.; Vekris, J. E. *Acta Crystallogr.* **1989**, C45, 1847.
- (19) Cameron, T. S.; Roobottom, H. K.; Dionne, I.; Passmore, J.; Jenkins, H. D. B. *Inorg. Chem.* **2000**, 39, 2042 and references therein.
- (20) Dionne, I. Presented at the 1998 CIC Conference in Whistler, BC, Canada, Abstract 591.
- (21) Murchie, M. P.; Passmore, J.; Sutherland, G. W.; Kapoor, R. *J. Chem. Soc., Dalton Trans.* **1992**, 503.
- (22) Cameron, T. S.; Deeth, R. J.; Dionne, I.; Jenkins, H. D. B.; Krossing, I.; Passmore, J.; Roobottom, H. *Inorg. Chem.* **2000**, 39, 5614.
- (23) Brownridge, S.; Krossing, I.; Passmore, J.; Jenkins, H. D. B.; Roobottom, H. K. *Coord. Chem. Rev.* **2000**, 197, 397.

- (6) (a) Stillings, M.; Symons, M. C. R.; Wilkinson, J. G. *J. Chem. Soc. A*, **1971**, 3201. (b) Symons, M. C. R. *J. Chem. Soc.* **1957**, 2440. (c) Ingram, D. J. E.; Symons, M. C. R. *J. Chem. Soc.* **1957**, 2437. (d) Chandra, H.; Ramakrishna Rao, D. N.; Symons, M. C. R. *J. Chem. Soc., Dalton Trans.* **1987**, 729.
- (7) Burns, R. C.; Gillespie, R. J.; Sawyer, J. F. *Inorg. Chem.* **1980**, 19, 1423.
- (8) (a) Burford, N.; Passmore, J.; Sanders, J. C. P. *From Atoms to Polymers, Isoelectronic Analogies*; Liebman, J. F., Greenberg, A., Eds.; Verlag Chemie: Weinheim, Germany, 1989; pp 53–108 and references therein. (b) Gillespie, R. J.; Passmore, J. *Adv. Inorg. Radiochem.* **1975**, 17, 49 and references therein. (c) Gillespie, R. J. *J. Chem. Soc. Rev.* **1979**, 8, 315.
- (9) Gardener, D. M.; Fraenkel, G. K. *J. Am. Chem. Soc.* **1956**, 78, 6411.
- (10) Applying an electric potential across the solution caused the blue species to move to the cathode.⁹
- (11) (a) Gillespie, R. J.; Passmore, J. *Chem. Commun.* **1969**, 1333. (b) Gillespie, R. J.; Passmore, J.; Ummat, P. K.; Vaidya, O. C. *Inorg. Chem.* **1971**, 10, 1327. (c) Davies, C. G.; Gillespie, R. J.; Park, J. J.; Passmore, J. *Inorg. Chem.* **1971**, 10, 2781.
- (12) Low, H. S.; Beaudet, R. A. *J. Am. Chem. Soc.* **1976**, 98, 3849.
- (13) Passmore, J.; Sutherland, G.; Taylor, P.; Whidden, T. K.; White, P. S. *Inorg. Chem.* **1981**, 20, 3839.
- (14) Thomaskiewicz, I.; Passmore, J.; Schatte, G.; Sutherland, G. W.; O'Hare, P. A. G. *J. Chem. Thermodyn.* **1994**, 26, 299 and references therein.



Therefore, $\text{S}_8(\text{AsF}_6)_2$ is lattice stabilized in the solid state.^{24,25} The presence of S_5^{+} in equilibrium with S_8^{2+} is not in doubt. However, it could be that the blue color^{26,27} is due to $\text{S}_3^{+}(\text{solv})$ (or $2\text{S}_3^{+}(\text{solv}) = \text{S}_6^{2+}(\text{solv})$, cf. Te_6^{2+} , $\text{S}_3\text{-Te}_3^{2+}$ ²⁸) rather than $\text{S}_5^{+}(\text{solv})$, both of which may be present according to eq 4. An MCD study²⁹ of sulfur oxidized by oleum showed the blue species to have axial symmetry, consistent with a highly fluxional $\text{S}_5^{+}(\text{solv})$, but the results are also entirely consistent with a D_{3d} symmetrical $10\pi \text{S}_6^{2+}(\text{solv})$ dication.

In this paper, we address the nature of the equilibrium of S_8^{2+} in solution (what is the unknown cation in eq 2?) and the identity of the blue species by calculating the energetics of possible equilibria by including solvation energies (SCIPCM model, COSMO model for selected equilibria) as well as calculating the UV–vis spectra of the species (CIS plus TD-DFT for selected cations) and comparing these with the observed spectra.

Computational Details

All calculations were performed using Gaussian94W and Gaussian98W.³⁰ Previous calculations of E_n^{2+} ($\text{E} = \text{S}, \text{Se}, n = 4, 8$)^{22,31,32} showed the particular strength of the hybrid HF-DFT level B3PW91^{33,34} in the description of homopolyatomic sulfur and selenium cations. The B3PW91 level mastered even problem cases such as S_8^{2+} ,³⁵ and thermodynamic calculations with B3PW91/6-311+G(3df)/B3PW91/6-311+G* reproduced the dimerization energy of $2\text{S}_2^{+} \rightarrow \text{S}_4^{2+}$ which with classical ab initio methods finally only converged at the extremely expensive CCSD(T)/cc-pV5Z level.³¹ The MP n levels ($n = 2, 3, 4$) gave oscillating energies for S_2^{+} and S_4^{2+} that did not converged even with a cc-pVQZ basis³¹ and were therefore not appropriate for the resolution of this

problem.³¹ Therefore, B3PW91 was selected to compute the properties of all species used here. Basis sets were used as implemented in Gaussian94.³⁰ Full optimizations (including frequency analysis) to determine stationary points were done with the 6-311+G* basis set, and Raman scattering activities were calculated using the option Freq=Raman in G98W; more accurate total energies for the comparison of the relative stabilities and the calculation of thermodynamic properties were obtained by single point calculations with B3PW91/6-311+G(3df) using the respective B3PW91/6-311+G* optimized structures. Nonscaled zero point energies (ZPEs) were included for all thermodynamic calculations, and derived enthalpies and free energies were corrected to 298 K. It should be pointed out that all given reactions are isodesmic (but not necessarily isogyric) with the same number and type of bonds on both sides of the equation which increases the credibility of the details of the calculated reaction enthalpies due to substantial error cancellation. Solvation enthalpies were approximated at the B3PW91/6-311+G* level in a self-consistent reaction field using a self consistent isodensity polarized continuum model (e.g., the option SCRF=SCIPCM).³⁶ All calculated free energies of dissociation in solution were corrected by adding the difference between the gas phase 0 K value at the B3PW91/6-311+G* level with the calculated free energy at 298 K including the ZPE at the B3PW91/6-311+G(3df)/B3PW91/6-311+G* level to the total energy of the SCIPCM calculation at the B3PW91/6-311+G* level, e.g., see the following for S_4^{2+} :

gas phase 0 K total energy
(B3PW91/6-311+G*): -1591.78727 H

free energy at 298 K including the ZPE (B3PW91/6-311+G
(3df)/B3PW91/6-311+G*): -1591.87598 H
difference: -0.08870 H

SCIPCM calculation
(DC = 14; B3PW91/6-311+G*): -1592.13083 H

corrected SCIPCM free energy at 298 K (including
ZPE): $-1592.13083 \text{ H} + -0.08870 \text{ H} = -1592.21953 \text{ H}$

A table containing all necessary total energies is deposited as Supporting Information. By using the same solvation enthalpy methodology throughout, a large amount of error cancellation can be expected on both sides of the equation. Although the absolute solvation energies may be in error, the relative solvation energies are expected to be reliable due to error cancellation. To further support this point, the free energies of solvation of selected cations (S_4^{+} , S_5^{+} , S_7^{+} , S_6^{2+} , and S_8^{2+}) were also assessed by single point calculations using the same cation geometries and the COSMO solvation model³⁷ at the B3PW91/6-311+G* level. A table containing the COSMO-solvation energies is deposited. The agreement between the SCIPCM and COSMO model is very good, and the COSMO corrected $\Delta G(\text{SO}_2)$ values for reactions 14, 16, 17, and 19 are included in parentheses in Table 1. The positions of the transitions in the UV–vis spectra and their oscillator strengths, of all cations, were calculated at the CIS/6-311G(2df) level using the optimized B3PW91 geometries. In order to establish the quality of the CIS calculations, the transitions and oscillator strengths of S_6^{2+} and S_4^{2+} were also calculated by using time dependent DFT calculations at the BP86/SV(P) level³⁸ with the program Turbo-

- (24) A further example for a lattice stabilized species is the $\text{S}_3\text{N}_2^{2+}$ dication, which dissociates in the gas phase to give SN^{+} and S_2N^{+} ($\Delta H = -400 \text{ kJ/mol}$), but undergoes a lattice enforced dimerization in the salt $\text{S}_3\text{N}_2(\text{AsF}_6)_2$, see ref 25.
- (25) Brooks, W. V. F.; Cameron, T. S.; Parsons, S.; Passmore, J.; Shriver, M. J. *Inorg. Chem.* **1994**, *33*, 6230.
- (26) However, Mamantov et al.²⁷ suggested that the blue color is due to S_8^{2+} itself.
- (27) Norvell, V. E.; Tanemoto, K.; Mamantov, G.; Klatt, L. N. *J. Electrochem. Soc.* **1981**, 1254.
- (28) (a) Beck, J. *Angew. Chem., Int. Ed. Engl.* **1994**, *33*, 163. (b) Beck, J. *Coord. Chem. Rev.* **1997**, *163*, 55.
- (29) Stevens, P. J. *Chem. Commun.* **1969**, 1496.
- (30) Frisch, M. J.; Trucks, G. W.; Schlegel, H. B.; Gill, P. M. W.; Johnson, B. G.; Robb, M. A.; Cheeseman, J. R.; Keith, T.; Petersson, G. A.; Montgomery, J. A.; Raghavachari, K.; Al-Laham, M. A.; Zakrzewski, V. G.; Ortiz, J. V.; Foresman, J. B.; Cioslowski, J.; Stefanov, B. B.; Nanayakkara, A.; Challacombe, M.; Peng, C. Y.; Ayala, P. Y.; Chen, W.; Wong, M. W.; Andres, J. L.; Replogle, E. S.; Gomperts, R.; Martin, R. L.; Fox, D. J.; Binkley, J. S.; Defrees, D. J.; Baker, J.; Stewart, J. P.; Head-Gordon, M.; Gonzalez, C.; Pople, J. A. *Gaussian 94*, revision E.3; Gaussian, Inc.: Pittsburgh, PA, 1995.
- (31) Jenkins, H. D. B.; Jitariu, L. C.; Krossing, I.; Passmore, J.; Suontamo, R. *J. Comput. Chem.* **2000**, *21*, 218.
- (32) Krossing, I.; Passmore, J. *Inorg. Chem.* **1999**, *38*, 5203.
- (33) Becke, A. D. *J. Chem. Phys.* **1993**, *98*, 5648.
- (34) Perdew, J. P.; Wang, Y. *Phys. Rev.* **1992**, *B45*, 13244.
- (35) Earlier investigations led to transannular bonds that were either much shorter or much longer than the experimental value (see refs 15, 54–56).

- (36) Foresman, J. B.; Keith, T. A.; Wiberg, K. B.; Snoonian J.; Frisch, M. J. *J. Phys. Chem.* **1996**, *100*, 16098.
- (37) Barone, V.; Cossi, M. *J. Phys. Chem. A* **1998**, *102*, 1995.

Table 1. Reaction Enthalpies and Free Energies of Dissociation Reactions of S_n^{2+} ($n = 4, 6, 8, 10$) and S_6^{4+} in the Gas Phase and in SO_2 Solution at 298 K [in kJ/mol]^b

eq	dissociation Reactions of S_8^{2+} [kJ/mol]	$\Delta_f H^{298}$ theor	$\Delta_f H^{298}$ expt ^a	$\Delta_f G^{298}$ theor	$\Delta_f G^{298}(SO_2)$ theor	$\Delta_f G^{298}(HF)$ theor	$\Delta_f G^{298}(\text{oleum})$ theor
10	$S_6^{2+}(g) \rightarrow 2S_3^+(g)$	−93		−157	+163		
11	$S_6^{2+}(g) \rightarrow 1/2[S_4^{2+}(g) + S_8^{2+}(g)]$	+1	−4	+2	−27		
12	$S_6^{2+}(g) \rightarrow 1/2S_4^{2+}(g) + S_4^+(g)$	−84	−114	−110	−14		
13	$S_6^{2+}(g) \rightarrow 2/3S_4^{2+}(g) + 2/3S_5^+(g)$	−58	−74 ^c	−78	−39		
14	$S_8^{2+}(g) \rightarrow 2S_4^+(g)$	−170	−207 ^c	−224	+25 (+20)	+41	+42
15	$S_8^{2+}(g) \rightarrow S_3^+(g) + S_5^+(g)$	−135	−136 ^c	−200	+68		
16	$S_8^{2+}(g) \rightarrow 1/2S_6^{2+}(g) + S_3^+(g)$	−89	−90	−121	−5 (−15)	+2	+2
17	$S_8^{2+}(g) \rightarrow 2/3S_6^{2+}(g) + 1/3S_5^+(g) + 1/3S_7^+(g)$	−30	−24	−51	+13 (+8)	+17	+17
18	$S_8^{2+}(g) \rightarrow 2/3S_6^{2+}(g) + 2/3S_6^+(g)$	−27	−12	−48	+19		
19	$S_8^{2+}(g) \rightarrow 3/4S_6^{2+}(g) + 1/2S_7^+(g)$	0	+3	−15	+23 (+19)	+24	+24
20	$S_{10}^{2+}(g) \rightarrow 2S_5^+(g)$	−268		−337	−80		
21	$S_6^+(g) \rightarrow 0.5[S_5^+(g) + S_7^+(g)]$	−4	−26 ⁸²	−4	−8		

^a Semiexperimentally derived values [$\Delta_f H^{298}(S_n^+, g)$: experimental values, $\Delta_f H^{298}(S_n^{2+}, g)$: calculated values], ^b Selected equilibria were also assessed using HF (DC = 83) and oleum (DC = 110) as a solvent and some also by using the COSMO model (values in parentheses). Exergonic free energies of reaction are printed in bold. ^c From ref 22.

Table 2. Experimental and Computed [CIS/6-311G(2df)//B3PW91/6-311+G* (S, Se); CIS/3-21G*//B3PW91/3-21G*(Te)] UV–Vis Spectra of E_4^{2+} (E = S, Se, Te) and E_8^{2+} (E = S, Se)^a

state	S_4^{2+} expt ^b	S_4^{2+} comp	Se_4^{2+} expt ^b	Se_4^{2+} comp	Te_4^{2+} expt ^b	Te_4^{2+} comp	Se_8^{2+} expt ^b	" S_8^{2+} " expt ^c	S_8^{2+} comp
1st exc	300–380 max 330 (ϵ 2150)	310 S (0.1182)	360–460 max 410 (ϵ 2150)	388 S (0.1059)	460–560 max 510 (ϵ 2300)	459 S (0.1226) 1810 T (0)	600–750 max 685 (ϵ 400)	500–700 max 585 (ϵ 2500) ^d	558 S (0.0005)
2nd exc		310 S (0.1182)		388 S (0.1059)		459 S (0.1226)			528 S (0.0713)
3rd exc		298 S (0)		369 S (0)	400–450 max 425 (ϵ 400)	457 S (0)	430–510 max 470 (ϵ 250)		500 S (0.0813)
4th exc	280 weak	285 S (0)		348 S (0)		425 S (0)			361 S (0.12)
5th exc		278 S (0)	290–340 max 320 (ϵ 170)	334 S (0)		388 S (0)	280–380 max 300 (ϵ 900)		325 S (0.03)
6th exc		278 S (0)		334 S (0)		383 S (0)			321 S (0.02)

^a Parentheses indicate oscillator strengths of transition. Also, for comparison, the main calculated transition (oscillator strength) of S_4^{2+} at the TD-DFT level is 318 nm ($f = 0.107$). ^b By oxidation of sulfur/selenium/tellurium with $S_2O_6F_2$ in HSO_3F .⁸³ ^c By dissolving $S_8(AsF_6)_2$ in HSO_3F .^{11,83} ^d Assuming the dissolved species was entirely S_8^{2+} .

Table 3. Calculated UV–Vis Transitions of Sulfur Cations [CIS/6-311G(2df)//B3PW91/6-311+G*]^a

cation sym state	S_2^+	$S_3^+ C_{2v}, {}^2B_2$	$S_3^+ C_{2v}, {}^2A_1$	$S_3^+ C_s, {}^2A'$	$S_3^{2+} D_{3h}, {}^3A_1'$	$S_6^{4+} D_{3h}, {}^1A_1'$
1st exc	2943 (0)	68417 (0)	4547 (0.0019)	2552 (0)	298 (0.0201)	409 (0)
2nd exc	694 (0.0001)	10681 (0)	1788 (0)	1892(0)	298 (0.0201)	409 (0)
3rd exc	562 (0)	3972 (0)	1558 (0.0003)	1348 (0.0004)	292 (0.0000)	373 (0)
4th exc	370 (0.0010)	2362 (0.0065)	1340 (0)	877 (0.0001)	292 (0.0000)	286 (0.0103)
5th exc	327 (0)	506 (0.0002)	532 (0)	359 (0.0199)	270 (0.0000)	286 (0.0103)
6th exc	296 (0)	436 (0)	460 (0) ^b	347 (0) ^c	252 (0.0000)	256 (0.0011)

^a Parentheses indicate oscillator strength of transition. ^b 7th exc 333 (0.1354). ^c 7th exc 324 (0.1506).

mole.³⁹ The agreement between CIS/6-311G(2df) and time dependent DFT calculations at the BP86/SV(P) level is excellent for the positions of the first excited state while the agreement of the calculated oscillator strengths of the transitions is only qualitative. TD-DFT excitation energies and oscillator strengths of S_6^{2+} and S_4^{2+} are included in Tables 2 and 4.

Computation of S_n^+ ($n = 3–7$), S_3^{2+} , S_6^{2+} , S_6^{4+} , and S_{10}^{2+}

A number of charged and neutral sulfur species were previously examined by ab initio methods, namely $S_2–$

S_{12} ,^{40,41} $S_2–S_{13}$,⁴² $S_5–S_8$,⁴³ detailed studies of S_4 ,^{44,45} an extensive CI-study on S_3^{2+} ,⁴⁶ various reports on S_4^{2+} –^{47–53} and S_8^{2+} ,^{16,22,54–56} (inter alia) reports on $S_3^+–S_6^+$,⁵⁷ and a detailed study of neutral, anionic, and cationic $S_3–S_5$ species.⁵⁸ The latter study showed the presence of very shallow S_n^+ ($n = 3–5$) hypersurfaces. Three S_3^+ isomers

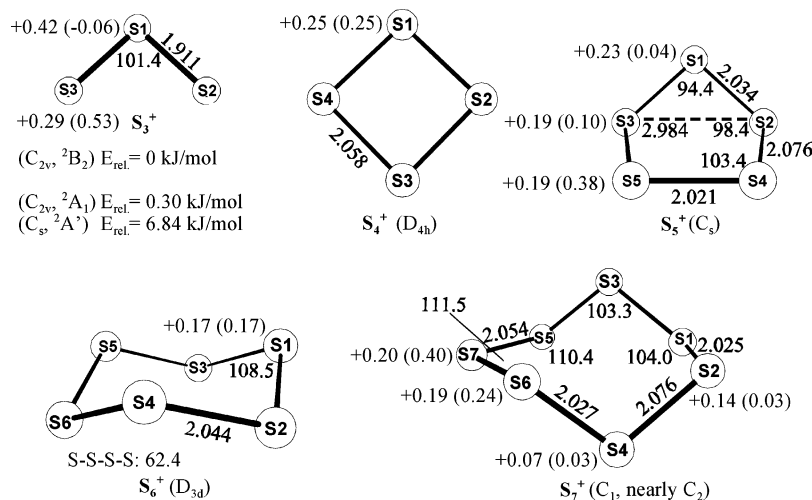
- (38) (a) Bauernschmitt, R.; Ahlrichs, R. *Chem. Phys. Lett.* **1996**, 256, 454. (b) Bauernschmitt, R.; Häser, M.; Treutler, O.; Ahlrichs, R. *Chem. Phys. Lett.* **1997**, 264, 573. (c) Eichkorn, K.; Weigend, F.; Treutler, O.; Ahlrichs, R. *Theor. Chim. Acta* **1997**, 97, 119. (39) TURBOMOLE, Version 5: (a) Ahlrichs, R.; Bär, M.; Häser, M.; Horn, H.; Kölmel, C. *Chem. Phys. Lett.* **1989**, 162, 165. (b) v. Arnim, M.; Ahlrichs, R. *J. Chem. Phys.* **1999**, 111, 9183.

- (40) Raghavachari, K.; Rohlfink, C. M.; Binkley, J. S. *J. Chem. Phys.* **1990**, 93, 5862. (41) Millefiori, S.; Alparone, A. *J. Phys. Chem. A* **2001**, 105, 9489. (42) Hohl, D.; Jones, R. O.; Car, R.; Parrinello, M. *J. Chem. Phys.* **1988**, 6823. (43) Cioslowski, J.; Szarecka, A.; Moncrieff, D. *J. Phys. Chem. A* **2001**, 105, 501. (44) Quelch, G. E.; Schaefer, H. F.; Marsden, C. J. *J. Am. Chem. Soc.* **1990**, 112, 8719. (45) Orlova, G.; Goddard, J. G. *J. Phys. Chem. A* **1999**, 103, 6825. (46) Marsden, C. J.; Quelch, G. E.; Schaefer, H. F. *J. Am. Chem. Soc.* **1992**, 114, 6802. (47) Tanaka, K.; Yamabe, T.; Terama, H.; Fukui, K. *Inorg. Chem.* **1979**, 18, 3591.

Table 4. Calculated UV–Vis Transitions of Sulfur Cations [CIS/6-311G(2df)//B3PW91/6-311+G*]^a

cation sym state	S ₄ ⁺ D _{4h} , ² B _{2u}	S ₅ ⁺ C _s , ² A''	S ₆ ⁺ D _{3d} , ² A _{1g}	S ₆ ²⁺ D _{3d} , ¹ A _{1g}	S ₇ ⁺ C ₁	S ₈ ²⁺ C _s , ¹ A'	S ₈ ²⁺ extrapolated ^b
1st exc	547 (0)	674 (0.0265)	1249 (0.0315)	564 (0.1233)	555 (0.0082)	558 (0.0005)	575 (€ 400)
2nd exc	547 (0)	420 (0.0093)	1249 (0.0315)	564 (0.1233)	477 (0.0071)	528 (0.0713)	
3rd exc	447 (0.0551)	373 (0.0030)	599 (0)	392 (0)	443 (0.0212)	500 (0.0813)	
4th exc	447 (0.0551)	361 (0)	599 (0)	392 (0)	374 (0.0057)	361 (0.1188)	395 (€ 250)
5th exc	395 (0)	344 (0.0080)	328 (0.0046)	303 (0)	341 (0.0005)	325 (0.0268)	
6th exc	388 (0) ^c	318 (0)	313 (0.0011)	295 (0.0028)	313 (0.0009)	321 (0.0172)	252 (€ 400)

^a Parentheses indicate oscillator strength of transition. Also, for comparison, the main calculated transitions (oscillator strengths) of S₆²⁺ at the TD-DFT level are 555 nm (0.052), 439 (0.018), and 299 (0.008). ^b Extrapolated from the experimental Se₈²⁺ spectrum (see Supporting Information). ^c 7th 328 (0.0008), 8th 326 (0), 9th 307 (0).

**Figure 3.** Optimized geometries, calculated Mulliken charges (spin densities) of all true S_n⁺ minima at the B3PW91/6-311+G* level of theory.

similar in energy but different in structure were found [*C*_{2v} (²A₁); *C*_{2v} (²B₂); *C*_s (²A')]. For S₄⁺ the D_{4h} symmetric square is clearly the global minimum, but for S₅⁺ the C_s symmetric five membered ring in the envelope conformation (²A'') is only slightly favored over a C₂ symmetric ring⁵⁸ and a D_{5h} symmetric ring is no minimum at the B3PW91 level (*E*_{rel} = +131 kJ/mol). Interestingly, it was shown that the triangular S₃²⁺ has a triplet ground state.⁴⁶ In previous reports we examined the properties of S₂⁺, S₄²⁺ (D_{4h}), and S₈²⁺ (C_s) at the B3PW91/6-311+G* level of theory.^{22,31,32} These geometries were used here together with an investigation of three states of S₃⁺, triangular S₃²⁺, C_s symmetric S₅⁺, D_{3d} symmetric S₆⁺, C_{2v}, D_{6h}, and D_{3d} symmetric S₆²⁺, D_{3h} symmetric S₆⁴⁺, asymmetric cyclic S₇⁺, and asymmetric tricyclic S₁₀²⁺ (with the Se₁₀²⁺ geometry). Previous calculations^{22,31,32} gave S–S bond distances 1.7–2.0% longer than the experimental values, and therefore, all given S–S distances were scaled by a factor of 1/1.0185 = 0.982. All

optimized geometries, except that of S₁₀²⁺, are shown in Figures 3 and 4 together with the respective Mulliken charges and spin densities (in parentheses) obtained with the large 6-311+G(3df) basis set.⁵⁹ Only the geometries of S₆²⁺ and S₁₀²⁺ are briefly discussed while a discussion of the geometries of all the other species is included in the Supporting Information which also includes a table of the (scaled) calculated vibrational frequencies (with Raman intensities and zero point energies).

C_{2v}, D_{6h}, or D_{3d} Symmetric S₆²⁺? A C_{2v} boat and D_{3d} chair conformation of the S₆ ring was assumed for the optimization of S₆²⁺ (see Supporting Information), as was the procedure for S₆⁺. In contrast to the experimentally observed heavier C_{2v} symmetric Te₆²⁺ dication,²⁸ a D_{3d} symmetric S₆²⁺ dication was found to be 18 kJ/mol lower in energy than the C_{2v} species. The S–S distance of 2.028 Å is shorter than that in S₆ and S₆⁺, the S–S–S bond angle α of 113.7° is larger, and the S–S–S–S torsion angle τ of 47.6° smaller (cf. S₆, 2.061 Å, α 103.0°, τ 73.1°; S₆⁺, 2.044 Å, α 108.5°, τ 62.4°). Therefore, the geometry of S₆²⁺ is best described as a flattened six membered ring in a chair conformation where the positive charges are delocalized over all atoms. Although the D_{3d} S₆²⁺ dication with 10 “π” electrons is not strictly planar and thus does not conform with the requirements for the (4*n* + 2)π electron Hückel-rule, an analysis of the molecular orbitals showed an almost complete separation of σ- and π-MOs, and therefore, we propose that

- (48) (a) Saethre, L. J.; Gropen, O. *Can. J. Chem.* **1992**, *70*, 348. (b) Gropen, O.; Saethre, L. J.; Wilsoff-Nielssen, E. *Studies in physical and theoretical chemistry*; Carbo, ed.; Elsevier: Amsterdam, 1982; p 427.
- (49) Kao, J. J. *Mol. Struct.* **1980**, *63*, 293.
- (50) Tang, T. H.; Bader, R. F. W.; McDougall, P. J. *Inorg. Chem.* **1985**, *24*, 2047.
- (51) Skrezenek, F. L.; Harcourt, R. D. *Theor. Chim. Acta* **1985**, *67*, 271.
- (52) Landwijk, G. V.; Janssen, R. A. J.; Buck, H. M. *J. Am. Chem. Soc.* **1990**, *112*, 4155.
- (53) Sannigrahi, M.; Grein, F. *Can. J. Chem.* **1994**, *72*, 298.
- (54) Baird, N. C. *J. Comput. Chem.* **1984**, *5*, 35.
- (55) Tang, T. H.; Bader, R. F. W.; MacDougall, P. J. *Inorg. Chem.* **1985**, *24*, 2047.
- (56) Cioslowski, J.; Gao, X. *Int. J. Quantum Chem.* **1997**, *65*, 609.
- (57) Pascoli, G.; Lavendy, H. *Int. J. Mass Spectrom.* **2001**, *206*, 153.
- (58) Zakrzewski, V. G.; von Niessen, W. *Theor. Chim. Acta* **1994**, *88*, 75.

- (59) It should be noted that for homopolyatomic sulfur cations NBO natural charges and Mulliken charges utilizing the 6-311+G(3df) basis set are virtually the same (±0.02), see refs 22 and 32.

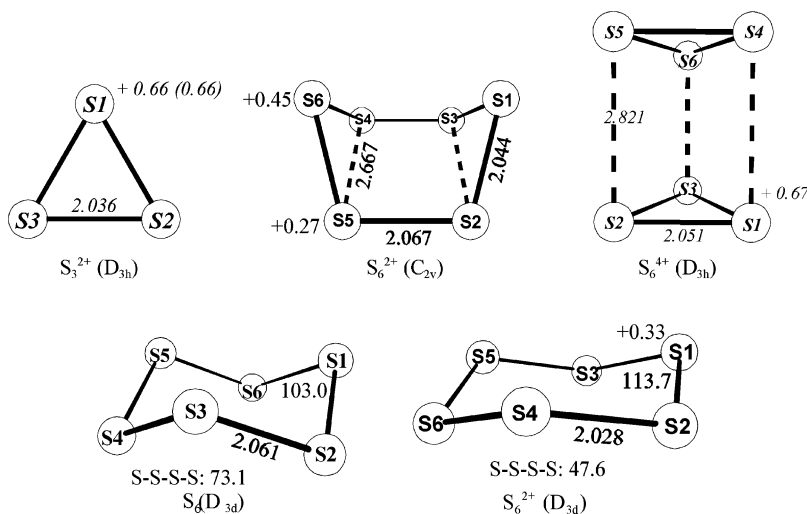


Figure 4. Optimized geometries, calculated Mulliken charges (spin densities [only S_3^{2+}]) of S_n^{2+} ($n = 3, 6$), S_6 , and S_6^{4+} at the B3PW91/6-311+G* level of theory.

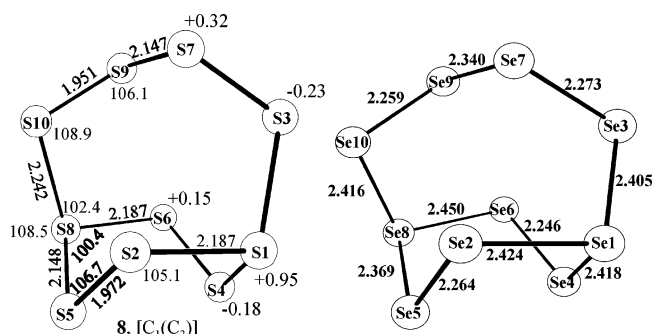


Figure 5. Comparison of the calculated structure of S_{10}^{2+} with the X-ray structure of the Se_{10}^{2+} dication in $[Se_{10}]^{2+}[SO_3F]^{-2}$.⁶¹

the D_{3d} isomer may be viewed as a 10π S_6^{2+} dication. A completely planar D_{6h} symmetric S_6^{2+} , which would be a true 10π Hückel aromatic, was also calculated and found to be higher in energy at +51 kJ/mol (B3PW91/6-311+G(3df)//B3PW91/6-311+G*). From the preceding, it follows that the slightly puckered D_{3d} symmetric S_6^{2+} is the global minimum of the examined S_6^{2+} isomers.

The geometry of the C_{2v} boat structure of S_6^{2+} is of interest for a comparison with the heavier homologous Te_6^{2+} dication. C_{2v} S_6^{2+} follows the same short–long–short bond alternation pattern (2.044–2.067–2.044 Å), as found experimentally in Te_6^{2+} (2.708–2.737–2.708 Å)_{av}.⁶⁰ It is a transition state with an imaginary frequency at 117i cm^{-1} . An optimization with the larger 6-311G(2df) basis set verified the geometry of C_{2v} S_6^{2+} and its assignment as a transition state [104i cm^{-1}].

The Geometry of S_{10}^{2+} . The calculated C_1 (but almost C_2) symmetric S_{10}^{2+} geometry and the experimental Se_{10}^{2+} structure⁶¹ in $[Se_{10}][SO_3F]_2$ are compared in Figure 5.

Calculated S_{10}^{2+} and experimental Se_{10}^{2+} geometries are in good qualitative agreement; all experimentally found features, such as bond lengths alternation, are also found in the computed structure of the lighter homologue.

(60) Average Te–Te bond lengths of the Te_6^{2+} dication in four published X-ray crystal structure determinations.²³

(61) (a) Collins, M. J.; Gillespie, R. J.; Sawyer, J. F.; Schrobilgen, G. J. *Acta Crystallogr.* **1986**, C42, 13. (b) Burns, R. C.; Chan, W.-C.; Gillespie, R. J.; Sawyer, J. F.; Slim, D. R. *Inorg. Chem.* **1980**, 19, 1432.

Computed Thermodynamic Properties

In order to utilize the experimentally determined enthalpies of formation of the gaseous sulfur monocations,⁶² all $\Delta_f H^{298}$ values of the S_n^{2+} ($n = 3, 4, 6, 8, 10$) dications employed in this study were calculated. $\Delta_f H^{298}$ of $S_4^{2+}(g)$ and $S_8^{2+}(g)$ were previously established as +2318 kJ/mol (S_4^{2+})³² and +2151 kJ/mol (S_8^{2+})²² so that only triplet- S_3^{2+} , S_6^{2+} , and S_{10}^{2+} were unknown. $\Delta_f H^{298}(S_3^+, g)$ was experimentally determined as 1076 kJ/mol.⁶² The second adiabatic ionization potential of $S_3(g)$ was calculated as 1462 kJ/mol, and so, $\Delta_f H^{298}(S_3^{2+}, g)$ follows according to eq 6:

$$\Delta_f H^{298}(S_3^{2+}, g) = \Delta_f H^{298}(S_3^+, g) + \text{second IP}(S_3, g) = 1076 + 1462 = +2538 \text{ kJ/mol} \quad (6)$$

Two different routes were used to establish $\Delta_f H^{298}$ of $S_6^{2+}(g)$. It is accessible from the calculated dissociation enthalpy of S_6^{2+} giving two S_3^+ (−93 kJ/mol, see below) and the published $\Delta_f H^{298}$ of $S_3^+(g)$ of 1076 kJ/mol⁶² (eq 6) or by calculating the combined $^{1+2}\text{IP}(S_6, g)$ (2130 kJ/mol) and adding the experimental $\Delta_f H^{298}(S_6, g)$ ⁶² (eq 7).

$$\Delta_f H^{298}(S_6^{2+}, g) = 2\Delta_f H^{298}(S_3^+) - \Delta_f H_{\text{diss}} = 2 \times 1076 - (-93) = +2245 \text{ kJ/mol} \quad (7)$$

$$\Delta_f H^{298}(S_6^{2+}, g) = 2\Delta_f H^{298}(S_6, g) + ^{1+2}\text{IP}(S_6, g) = 102 + 2128 = +2230 \text{ kJ/mol}$$

$$\Rightarrow \text{average } \Delta_f H^{298}(S_6^{2+}, g) = (2245 + 2230)/2 = 2238 \text{ kJ/mol}$$

The enthalpy of formation of gaseous S_{10}^{2+} was assessed from the known, experimentally determined $\Delta_f H^{298}(S_5^+, g)$ of 939 kJ/mol and the calculated dissociation enthalpy of S_{10}^{2+} giving two S_5^+ of −268 kJ/mol (see below).

(62) (a) Wagman, D. D.; Evans, W. H.; Parker, V. B.; Schumm, R. H.; Halow, I.; Bailey, S. M.; Churney, K. L.; Nuttal, R. L. *J. Phys. Chem. Ref. Data* **1982**, 11, Suppl. 2. (b) Lias, S. G.; Bartmess, J. E.; Liebman, J. F.; Holmes, J. L.; Levin, R. D.; Mallard, W. G. *J. Phys. Chem. Ref. Data* **1988**, 17, Suppl. 1.

$$\Delta_f H^{298}(\text{S}_{10}^{2+}, \text{g}) = 2\Delta_f H^{298}(\text{S}_5^{+}, \text{g}) - \Delta_r H_{\text{diss}} = 2 \times 939 - (-268) = +2146 \text{ kJ/mol} \quad (9)$$

This gives $\Delta_f H^{298}(\text{S}_{10}^{2+}, \text{g})$ as 2146 kJ/mol and only slightly lower than the value found for S_8^{2+} . All derived enthalpies of formation of the polysulfur dications increase with increasing average charge per atom and follow the (expected) ordering of $\Delta_f H^{298}(\text{S}_3^{2+}, \text{g}) > \Delta_f H^{298}(\text{S}_4^{2+}, \text{g}) > \Delta_f H^{298}(\text{S}_6^{2+}, \text{g}) > \Delta_f H^{298}(\text{S}_8^{2+}, \text{g}) > \Delta_f H^{298}(\text{S}_{10}^{2+}, \text{g})$ or 2538 > 2318 > 2238 > 2151 > 2146 kJ/mol.

Gas-Phase Dissociation Reactions of S_n^{2+} ($n = 4, 6, 8, 10$)

Accurate total energies of all the S_n^{+} ($n = 2-7$) and S_n^{2+} ($n = 3, 4, 6, 8, 10$) species were obtained by single point calculations at the B3PW91/6-311+G(3df)//B3PW91/6-311+G* level. This procedure allowed us to estimate the gas phase energetics of possible dissociation reactions of S_8^{2+} on a purely theoretical basis (labeled “theor” in Table 1). The semiexperimentally^{63,64} obtained values from ref 22 are included for comparison and agree with the theoretically obtained values. The largest deviation (37 kJ/mol⁶⁵) was found for the formation of 2 $\text{S}_4^{+}(\text{g})$ in eq 14 and may be due to the incorrect enthalpy of formation of gaseous S_4 ;⁶⁵ all the other values of calculated and semiexperimental enthalpies are closer, with a maximum deviation of 18 kJ/mol.⁶⁵ We restricted Table 1 to likely dissociation reactions; i.e., the formation of S_2^{+} and S_4^{2+} , which were experimentally shown¹⁸⁻²⁰ to be highly improbable, was excluded. However, in the oxidation of sulfur by AsF_5 with trace halogen present, the S_4^{2+} stage can be reached,¹⁸ and therefore, we included the two most favorable dissociation reactions involving the presence of S_4^{2+} (eqs 12 and 13). Additional dissociation reactions are provided in the Supporting Information. Entropy favors the dissociation of S_n^{2+} , and therefore, we used the free energies of the respective reactions in the discussion of the dissociation behavior, included in Table 1.

According to the calculation, all the doubly charged $\text{S}_n^{2+}(\text{g})$ ($n = 4, 6, 8, 10$) species are unstable toward the formation of smaller, less charged fragments $\text{S}_n^{+}(\text{g})$ ($n = 2-7$) by 93–268 kJ/mol ($\Delta_r H$, see Table 1 and Supporting Information). $\text{S}_6^{2+}(\text{g})$ is considerably more stable toward a symmetric cleavage (into 2 $\text{S}_3^{+}(\text{g})$) than is $\text{S}_4^{2+}(\text{g})$, $\text{S}_8^{2+}(\text{g})$, or $\text{S}_{10}^{2+}(\text{g})$

[$\Delta_r H_{\text{diss}}$: -93 ($\text{S}_6^{2+}(\text{g})$) kJ/mol vs -258 ($\text{S}_4^{2+}(\text{g})$) kJ/mol, -170 ($\text{S}_8^{2+}(\text{g})$) kJ/mol, and -268 ($\text{S}_{10}^{2+}(\text{g})$) kJ/mol].

Solution Behavior of S_n^{2+} ($n = 4, 6, 8, 10$)

Reliable experimental solvation energies of species in nonaqueous systems are very difficult to obtain, especially for highly reactive species such as the sulfur homopolyatomic cations. The calculation of solvation energies by the polarized continuum models (PCM models) has increasingly been used within the last few years,^{66,67} and this method was shown to give reliable solvation energies if relative values are compared throughout. Therefore, the PCM models suggested themselves as a possible resolution, especially since also hypothetical species for which no experimental values were available had to be assessed. Moreover, polyatomic sulfur cations with the positive charge delocalized over all atoms in the weakly coordinating solvent SO_2 were modeled, and therefore, strong coordination of solvent molecules by the cations is highly unlikely. Therefore, we are confident that conclusions drawn from the calculated thermodynamics with inclusion of the solvation energies hold and give meaningful answers.

The inclusion of approximate solvation energies by a SCIPCM³⁶ model drastically changes most of the free energies of reaction. Calculated free reaction energies in SO_2 solution (DC = 14 at 298 K⁶²) are included in Table 1. Selected equilibria were also assessed in HF (DC = 83 at 298 K⁶²) and oleum (DC = 110 at 298 K⁶²) solution. If not stated otherwise, we only refer in the following sections to the free energies of reaction in SO_2 [$=\Delta_r G^{298}(\text{SO}_2)$].

S_8^{2+} Dissociation Reactions. Although the exclusive formation of $\text{S}_n^{+}(\text{g})$ ($n = 2-7$) monocations from $\text{S}_8^{2+}(\text{g})$ is highly favored in the gas phase, the solvation energy of the $\text{S}_8^{2+}(\text{SO}_2)$ dication is sufficiently high to outweigh the gas phase dissociation energy and make all these equations endergonic by at least 22 kJ/mol (see Table 1 and Supporting Information). Equation 15 shows that $\text{S}_8^{2+}(\text{SO}_2)$ does not simply dissociate into $\text{S}_3^{+}(\text{SO}_2)$ and $\text{S}_5^{+}(\text{SO}_2)$ as proposed in eq 4 above (endergonic in SO_2 by +68 kJ/mol). All dissociation reactions of $\text{S}_8^{2+}(\text{SO}_2)$ including the formation of a doubly charged $\text{S}_n^{2+}(\text{SO}_2)$ cation ($n = 4, 6$) are more favored than those giving only monocations. The most favored and the only exergonic reaction of this series (with the exclusion of those that include the formation of S_4^{2+}) is eq 16 (-5 kJ/mol). A graphic representation of the free energies of selected equilibria of the dissociation of S_8^{2+} in solvents with dielectric constants between 1 and 30 is given in Figure 6.

- (63) Semiexperimentally derived values of some equilibria were published earlier on the basis of the calculated $\Delta_f H^{298}$ of $\text{S}_n^{2+}(\text{g})$ ($n = 4, 8$) and the experimentally determined $\Delta_f H^{298}$ of all the $\text{S}_n^{+}(\text{g})$ ($n = 2-7$) radical cations. All new equilibria were assessed using the same procedure as in ref 22 and the above derived $\Delta_f H^{298}$ values of gaseous S_3^{2+} , S_6^{2+} , and S_{10}^{2+} .
- (64) In the case of S_4^{+} , we showed that the published appearance potential stems from the fragmentation of S_6 giving S_4^{+} and S_2 . We derived $\Delta_f H^{298}(\text{S}_4^{+}, \text{g})$ as 972 kJ/mol, see ref 32.
- (65) The larger differences occur in reactions including the $\text{S}_4^{+}(\text{g})$ radical cation. This is due to the differences in the respective $\Delta_f H^{298}$ of $\text{S}_4^{+}(\text{g})$. The published $\Delta_f H^{298}(\text{S}_4^{+}, \text{g})$ is +146 kJ/mol whereas the calculation of this property according to $\text{S}_8(\text{g}) = 2\text{S}_4(\text{g}) + \Delta_r H$ utilizing the experimental $\Delta_f H^{298}(\text{S}_8, \text{g})$ of 101 kJ/mol⁶² gives a value of $\Delta_f H^{298}(\text{S}_4, \text{g})$ of 164 kJ/mol. This difference of 18 kJ/mol adds up to 36 kJ/mol when examining eq 6 explaining the different values obtained.

- (66) Thomasi, J.; Persico, M. *Chem. Rev.* **1994**, *84*, 2027.

- (67) A literature search with the program Scifinder (CAS database) in mid 2001 gave 694 hits for the term “polarizable continuum model” mainly originating from the past few years. This shows the now widely accepted use of these models. Some selected successful (inorganic) applications of the PCM models approximating non aqueous solvents are found in: (a) Lanza, G.; Fraga, I. L.; Marks, T. J. *J. Am. Chem. Soc.* **2000**, *122*, 12764. (b) Castejon, H.; Wiberg, K. B.; Sklenak, S.; Hinz, W. *J. Am. Chem. Soc.* **2001**, *125*, 6092. (c) Perez, P.; Torre-Labbe, A.; Contreras, R. *J. Am. Chem. Soc.* **2001**, *123*, 5527. (d) Saint-Martin, H.; Vicent, L. E. *J. Phys. Chem. A* **1999**, *103*, 6862.

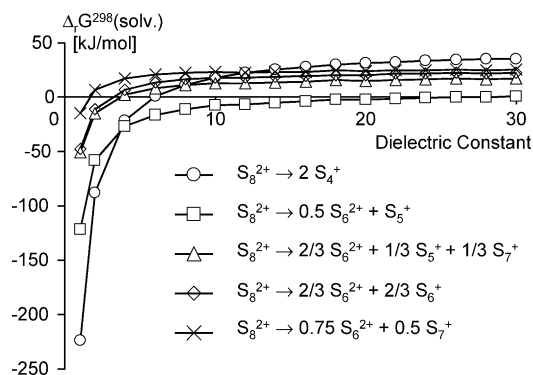


Figure 6. Solvent dependence of the calculated free energies of the dissociation of S_8^{2+} into S_6^{2+} and radical cations S_n^+ ($n = 5-7$) [in kJ/mol at 298 K].

Analysis of Figure 6 shows that nonpolar solvents favor the dissociation of S_8^{2+} to sulfur monocations as the overall solvation energies decrease with decreasing dielectric constant. The same holds for S_4^{2+} and S_6^{2+} (see Supporting Information).

S_6^{2+} Dissociation Reactions. The disproportionation of $S_6^{2+}(SO_2)$ to give $S_4^{2+}(SO_2)$ and $S_n^+(SO_2)$ ($n = 4, 5$; eqs 12 and 13) is endergonic by -14 to -39 kJ/mol, and the disproportionation of $S_6^{2+}(SO_2)$ giving $S_4^{2+}(SO_2)$ and $S_8^{2+}(SO_2)$ (-27 kJ/mol, eq 11) is the most endergonic of all the S_6^{2+} or S_8^{2+} dissociation reactions assessed, but all are kinetically forbidden. They may occur in mixtures where trace amounts of halogens or facilitating agent are present which allow the formation of the $S_4^{2+}(SO_2)$ cation.^{18a-d,21} In the absence of facilitating agent, the highest oxidation state achieved by reaction of S_8 with AsF_5 and SbF_5 is S_8^{2+} and its dissociation products whereas the formation of $S_4^{2+}(SO_2)$ was never observed.

Lower Average Oxidation States than S_8^{2+} . The formation of gaseous $S_{10}^{2+}(g)$ from $S_8^{2+}(g)$ and $2/8 S_8(g)$ is favorable by 30 kJ/mol; however, in SO_2 solution the dissociation of $S_{10}^{2+}(SO_2)$ to give $2S_5^+(SO_2)$ is highly favored by 80 kJ/mol and renders the presence of this isomer of the $S_{10}^{2+}(SO_2)$ dication in solution very unlikely. Reactions of $S_8^{2+}(SO_2)$ and neutral octasulfur $S_8(SO_2)$ to give $S_4^+(SO_2)$, $S_5^+(SO_2)$, and $S_7^+(SO_2)$ are very favorable by 13–58 kJ/mol (Supporting Information). Calculated free energies of reactions providing the $S_6^+(SO_2)$ cation would also be favorable, but $S_6^+(SO_2)$ itself is slightly unstable toward a disproportionation to give $S_5^+(SO_2)$ and $S_7^+(SO_2)$ by 8 kJ/mol (eq 21).

Calculated UV–Vis Spectra

The UV–vis spectra of S_n^+ ($n = 2-7$), S_n^{2+} ($n = 3, 4, 6, 8, 10$), and S_6^{4+} were calculated at the CIS/6-311G(2df) level of theory. Transitions of the singlet (dications) or doublet (monocations) ground state into the first six excited states were considered (for S_3^{2+} with a triplet ground state: triplet states); however, for species with low lying excited states such as S_3^+ the transitions into the first 9 excited states were calculated. The UV–vis spectra of the experimentally well characterized E_4^{2+} dications ($E = S, Se, Te$) were calculated and compared to the experimental results (see Table 2). Only

the relatively small 3-21G* basis set was used for Te_4^{2+} . To establish the quality of the CIS calculations for these species, the UV–vis spectra of S_4^{2+} and S_6^{2+} were also calculated by time dependent DFT calculations at the BP86/SV(P) level (Tables 2 and 4).^{38,39}

Calculated and experimental UV–vis spectra of E_4^{2+} ($E = S, Se, Te$) agree within -6% (S, Se) and -10% (Te); see Table 2. All calculated transitions are found at slightly higher energy than the experimental values; calculated oscillator strengths (f) and experimental extinction coefficients (ϵ) agree. Also, the TD-DFT calculation of S_4^{2+} gives very similar results to CIS as well as the experiment (CIS, 310 nm ($f = 0.1182$) vs TD-DFT, 318 nm ($f = 0.107$); expt, 330 nm ($\epsilon = 2500$)^{11c}). These initial investigations suggest that the CIS/6-311G(2df) level of theory should be capable of reproducing experimental UV–vis spectra of homopolyatomic chalcogen cations with an approximate error of -6 to -10% . Similarly, the UV–vis absorption of S_4 was earlier calculated to occur at 500 nm (using CIS),⁴⁴ 30 nm lower than the experimental value of 530 nm. Therefore, we are confident that, for all species in question, at least the calculated UV–vis transitions into the lower excited states are in good qualitative agreement with the experimentally expected absorptions. All calculated UV–vis spectra of the S_n^+ ($n = 2-7$) and S_n^{2+} ($n = 3, 6, 8$) are collected in Tables 3 and 4.

Experimental UV–vis spectra of isolated sulfur monocations S_n^+ ($n = 2-7$) are, to the best of our knowledge, not available to establish the quality of these computations. For S_3^+ a series of transitions into the low lying excited states was calculated, and the first intense expected transition, albeit into the 7th excited state, was calculated to occur at high energy at about 330 nm ($f = 0.13-0.15$). The transition into the first excited state of S_3^{2+} was calculated to occur at 298 nm, consistent with the slightly lower energy of the respective transition in S_4^{2+} (calcd 310 nm, $f = 0.12$), and in agreement with this picture, S_6^{2+} has a similarly intense ($f = 0.1233$) calculated transition at even lower energy at 564 nm. TD-DFT calculations on S_6^{2+} confirmed this assignment (555 nm, $f = 0.052$). The calculated UV–vis spectrum of S_5^+ shows two weak bands at 674 nm ($f = 0.0265$) and 420 nm ($f = 0.0093$), while S_4^+ has a medium transition at 447 nm ($f = 0.0551$), S_6^+ has one at 1249 nm ($f = 0.0315$), and S_7^+ has four weaker transitions between 374 ($f = 0.0057$) and 555 ($f = 0.0082$) nm.

Discussion

The Identity of the Unknown Species in Equation 2 from the Calculated Solution Thermodynamics. The most favored dissociation reactions of S_8^{2+} in solution, not involving the kinetically inaccessible S_4^{2+} and S_2^{2+} , are those leading to S_6^{2+} as a product. These are reactions 16–19 in Table 1, the most favorable of which is reaction 16 (eq 2 above) giving $1/2 S_6^{2+}$ and S_5^+ . Using the SCIPCM (COSMO) method to calculate solvation energies in $SO_2(l)$, ΔG (eq 16) is $-5(-15)$ kJ/mol, and in solutions of high dielectric constants such as HF or oleum, ΔG (eq 16) is $+2$ kJ/mol. Reaction 15 that gives S_5^+ and S_3^+ is significantly higher in

energy ($\Delta G_{(\text{SO}_2)} = +68\text{kJ/mol}$), strong evidence that the unknown in eq 2 above is not S_3^+ . The second most favorable dissociative reaction of S_8^{2+} is that by eq 17 giving $2/3\text{S}_6^{2+} + 1/3\text{S}_5^+ + 1/3\text{S}_7^+$ ($\Delta G_{(\text{SO}_2)} = +13(+8)$). However, it cannot be the most important dissociative route as the observed concentration^{7,17} of S_5^+ is much greater than that of S_7^+ , although it accounts for the presence^{7,17} of S_7^+ in small amounts. There is no experimental evidence for S_4^+ in systems that exclude facilitating agents (but see below); therefore, dissociation by eq 14 that is moderately unfavorable ($\Delta G_{(\text{SO}_2)} = +25(+20)$) can be excluded. Thus, these computational results reflect the known evidence from ESR studies.

The Identity of the Blue Species from a Comparison of the Experimental and Calculated UV–Vis Spectrum of S_8^{2+} and Its Dissociation Products. The spectrum of S_8^{2+} obtained in HSO_3F , shown in trace B in Figure 1, is similar to the spectrum in SO_2 , obtained by oxidation of S_8 with AsF_5 , shown in Figure 2, trace C, i.e., after addition of sufficient AsF_5 to oxidize the sulfur to S_4^{2+} , except for differences in intensities of their high energy tails.⁶⁸ This is because the oxidation in SO_2 was carried out in the absence of facilitating agent and the maximum oxidation state of sulfur obtained under these conditions is S_8^{2+} .^{18a–c,21} The spectrum in SO_2 shown in Figure 2, trace B, with sufficient AsF_5 to oxidize sulfur to S_8^{2+} is very dissimilar to the spectrum in HSO_3F (Figure 1, trace B), likely due to reactions of the dilute solution with surface and solvent impurities (see footnote 70). Thus, we take the experimentally observed spectrum of S_8^{2+} in HSO_3F to be that given in Figure 1, trace B, and in $\text{SO}_2(\text{l})$ shown in Figure 2, trace C. It was pointed out by Gillespie⁷ et al. that the experimental blue

UV–vis spectrum of S_8^{2+} is very different from the spectrum expected by extrapolation from the observed spectrum of Se_8^{2+} (given in Table 4), which has been unambiguously identified in solution by ^{77}Se NMR as a rigid molecule, at least at -70°C .⁶⁹ This implies that the solutions contain more than S_8^{2+} , if they contain this at all. Finally, although solid $\text{S}_8(\text{AsF}_6)_2$ is dark blue, we have prepared highly crystalline single crystals²² that are red in transmitted light, demonstrating that S_8^{2+} itself is not blue and therefore not the source of the blue solutions.

The theoretical calculations of the UV–vis spectra at both levels of theory used give reliable excitation frequencies (ca. $\pm 30\text{ nm}$) to the first excited states, the accuracy of those for the higher states decreasing with increase in energies. The oscillator strengths for the first excited states at these levels of theory are less accurate, but are at least approximate, and decrease in reliability for the higher excited states. Thus, the reliability of these calculations to simulate the UV–vis spectrum of S_3^+ is low as only high order transitions are expected in this region. Notwithstanding this cautionary note, its calculated spectrum is consistent with its absence. However, its presence can be excluded from the relatively more accurate calculation of the thermodynamics of the dissociation of S_8^{2+} in solution given above. Fortunately, all the first excitation frequencies of S_n^+ $n = 4, 5, 7, \text{S}_6^{2+}$, and S_8^{2+} (Table 3), lie in the critical 500–700 nm region. These are the most probable cations present in solution as implied by the thermodynamic calculations and previous experimental findings. The calculated frequency that is nearest to the experimentally found maximum at 585 nm is that calculated for S_6^{2+} (CIS at 564 nm, TD-DFT at 555 nm). It also has the highest calculated oscillator strength (CIS 0.123, TD-DFT 0.052), and the transition is doubly degenerate. The corresponding calculated (CIS) frequency (oscillator strength) for S_5^+ is at 674 nm (0.0265) and for S_8^{2+} (558 nm, 0.0005). Therefore, the calculations of the UV–vis spectra are entirely consistent with the presence of S_6^{2+} and imply that it could be largely responsible for the blue color of these solutions, rather than S_5^+ as previously claimed. We simulated the UV–vis spectra of stoichiometric mixtures of S_8^{2+} , S_6^{2+} , and S_5^+ in equilibrium with one another according to eq 16 at various ratios of $\text{S}_8^{2+}/0.5\text{S}_6^{2+} + \text{S}_5^+$. The calculated (CIS) oscillator strengths were used as a measure of the intensities.⁷¹ The figure is included in the Supporting Information. A comparison of the various calculated spectra compared with the experimental spectrum of S_8^{2+} in HSO_3F shown in Figure 1, trace B, implies that the solutions only contain a small amount of S_8^{2+} , and even less in SO_2 solution (see Table 5). These results are not substantially altered if the values for the excitation frequency and oscillator strength determined for S_6^{2+} by the TD-DFT method are used. Further support for the extensive dissociation of S_8^{2+} in solution is given from the values of the equilibrium constants (8.0 SO_2 ,

(68) The high energy tail at about 330 nm is absent in the HSO_3F spectrum and as yet could not be assigned. For the reasons given in the text, S_4^{2+} was excluded as a contributor. Another possible player would be AsF_3 as well as AsF_5 adducts thereof; however, AsF_3 was shown to absorb in the vacuum ultraviolet below 200 nm and not at 330 nm. Another possible assignment would be $\text{AsF}_3(\text{SO}_2)$: complexation of SO_2 by AsF_5 could red-shift the 280 nm band of SO_2 to lower energies. However, this remains a hypothesis as the experimental UV–vis spectrum of $\text{AsF}_3(\text{SO}_2)$ is unknown.

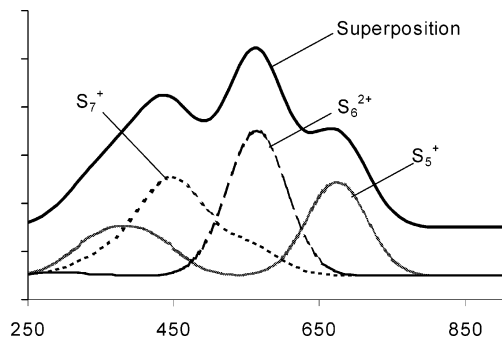
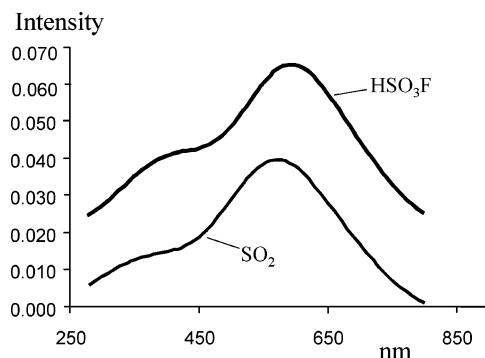
(69) Burns, R. C.; Collins, M. J.; Gillespie, R. J.; Schrobilgen, G. J. *Inorg. Chem.* **1986**, *25*, 4465.

(70) At the stoichiometric “ S_8^{2+} ” oxidation stage (i.e., sufficient AsF_5 added to oxidize sulfur to S_8^{2+}), the experimental UV–vis spectrum in SO_2 contained more bands (B in Figure 2) than the spectrum in HSO_3F , and from the ESR spectrum, S_5^+ and S_7^+ are present at about equal amounts.⁷ However, it is not likely that a stoichiometric amount of S_8^{2+} was actually present since the solution used for UV–vis spectroscopy was very dilute. The cell used had a path length of 0.5 cm compared with that in the $\text{HSO}_3\text{F}/\text{S}_8(\text{AsF}_6)_2$ experiment of as low as 0.005 cm; i.e., the HSO_3F solutions were about 100 times more concentrated than the SO_2 solution decreasing the effect of impurities and surface OH groups. Under these conditions, some of the added AsF_5 has been used in reacting with traces of impurities in the SO_2 and with the surfaces, and the UV–vis spectrum B is similar to that expected for “ S_{10}^{2+} ” or “ S_{11}^{2+} ”. Thus, the spectrum of S_8^{2+} in fluorosulfuric acid shown in Figure 1 is experimentally more reliable than that obtained on oxidation of sulfur by AsF_5 in SO_2 and shown as trace B in Figure 2. In addition to the higher concentration of $\text{S}_8(\text{AsF}_6)_2$ in the experiment with HSO_3F as a solvent, the method passivates the glass surfaces. Some solution was added to the rigorously dried 1.0 cm cell in the drybox, a spacer was slowly inserted into the cell forcing solution over the glass surfaces up above the insert and away from the spectrometer beam. At first, the blue solution was seen to decrease in intensity as it passed over the surfaces, but this ceased as more solution moved up the cell (J. Passmore, cf. ref 11).

(71) The simulated spectrum was obtained by a superposition of Gauss functions of type $f\sqrt{\frac{0.001}{\pi}}\exp(-0.001(x - t)^2)$ where f is the calculated oscillator strengths and t is the calculated position of the transition in question in nanometers.

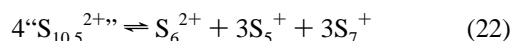
Table 5. Effect of Dilution on the Equilibrium $S_8^{2+} \rightleftharpoons 0.5S_6^{2+} + S_5^+$ in SO_2 ($K = 8.0$) and HSO_3F ($K = 0.4$) for Given S_8^{2+} Concentrations

given $[S_8^{2+}]$ [mol L ⁻¹]	corresponding $[S_6^{2+}]$ in SO_2 [mol L ⁻¹]	corresponding $[S_5^+]$ in SO_2 [mol L ⁻¹]	molar ratio $S_8^{2+}:S_5^+$	corresponding $[S_6^{2+}]$ in HSO_3F [mol L ⁻¹]	corresponding $[S_5^+]$ in HSO_3F [mol L ⁻¹]	molar ratio $S_8^{2+}:S_5^+$
1.000	2.518	5.036	1:5.0	0.348	0.695	1:0.7
0.100	0.543	1.085	1:10.9	0.749	0.150	1:1.5
0.010	0.117	0.234	1:23.4	0.016	0.032	1:3.2
0.0025	0.046	0.093	1:37.2	0.006	0.013	1:5.1
0.001	0.025	0.050	1:50.0	0.004	0.007	1:7.0

**Figure 7.** Simulated⁷¹ UV-vis spectrum of “ $S_{10.5}^{2+}$ ” including the contributions of the constituting S_6^{2+} , S_5^+ , and S_7^+ ions approximately resembling the experimental spectrum given⁷⁰ as S_8^{2+} (trace B) in Figure 2⁷ in the 400–800 nm region.**Figure 8.** Simulated⁷¹ UV-vis spectrum of the equilibrium mixture of solvated S_8^{2+} in HSO_3F and SO_2 at a given S_8^{2+} concentration of 0.001 mol/L (see Table 5 and ref 72).

0.4 HSO_3F) for eq 16 derived from the calculated free reaction energies of -5 kJ/mol in $SO_2(l)$ and $+0.4$ kJ/mol in HSO_3F . Dilution as in the UV-vis experiments further favors the formation of $1/2 S_6^{2+}$ and S_5^+ by dissociation of S_8^{2+} (see Table 5).

The observed spectrum in sulfur dioxide in Figure 2, trace B, that supposedly corresponded to the “ S_8^{2+} ” oxidation stage, can be approximated by the simulated⁷¹ spectrum of “ $S_{10.5}^{2+}$ ” containing S_6^{2+} , S_5^+ , and S_7^+ in Figure 8 (see footnote 70) with the later two radicals in equal concentration as given by eq 22, in agreement with the ESR spectrum⁷ and shown in Figure 7.



The experimental UV-vis spectrum of S_8^{2+} is attributable to a superposition of the absorption spectra of S_6^{2+} and S_5^+ with some S_8^{2+} in HSO_3F , but almost exclusively S_6^{2+} and S_5^+ in SO_2 . Figure 8 shows the simulated UV-vis spectrum⁷¹ of the calculated equilibrium mixture of these species in HSO_3F and SO_2 [given S_8^{2+} concentration: 0.001 mol/L (cf.

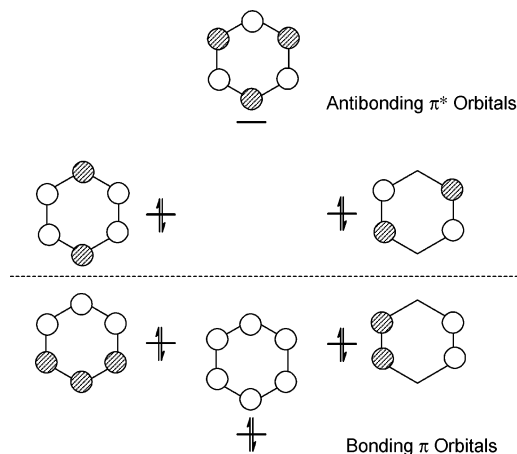
**Figure 9.** A view of the S_6^{2+} molecular orbitals of π and π^* symmetry perpendicular to the mean ring plane. The HOMO–LUMO transition of $\pi^*-\pi^*$ symmetry is likely largely responsible for the intense blue color of S_6^{2+} in solution (neglecting the nonplanarity of S_6^{2+} and the small mixing of MOs of σ - and π -symmetry, see above).

Table 5)].⁷² The simulated spectra do not change drastically if the TD-DFT results for S_6^{2+} are used.

The simulated spectra are in very good agreement with the experimental spectrum in HSO_3F (trace B in Figure 1) and that in SO_2 at the “ S_4^{2+} ” stage as obtained by the oxidation of sulfur with excess AsF_5 (trace C in Figure 2; no facilitating agent added, i.e., only the S_8^{2+} oxidation stage is reached even although excess AsF_5 is present), if the high energy bands in the experimental spectra are excluded. The extinction coefficient of the 585 nm band was found to be 2500 assuming it was due to S_8^{2+} . As our calculations suggest it to be largely due to S_6^{2+} , given eq 16 and complete dissociation, the extinction coefficient of the calculated 564 nm transition of S_6^{2+} should be about 5000.

The calculated oscillator strength and approximate extinction coefficient of the D_{3d} symmetric 10π S_6^{2+} (calcd, 564 (555) nm, $f = 0.1233$ (0.052); rough experimental estimation $\epsilon \approx 5000$) are similar to that of the 6π S_4^{2+} (calcd, 310 (318) nm, $f = 0.1183$ (0.107); experimental $\epsilon = 2150$). From the calculations, we suggest that the electronic transition responsible for the blue color of S_6^{2+} is of $\pi^*-\pi^*$ nature and the idealized S_6^{2+} molecular orbitals of π and π^* symmetry are shown in Figure 9 (neglecting the nonplanarity of S_6^{2+} and the small mixing of MOs of σ - and π -symmetry, see above).⁷³

As far as we are aware, there are no related sulfur rich 9π radicals to which the calculated oscillator strength of S_5^+

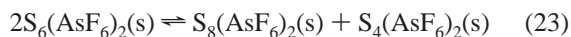
(72) This was about the concentration of the HSO_3F sample.^{11,70} The SO_2 sample was more dilute additionally favoring S_6^{2+} and S_5^+ formation.

(73) Our calculated π MOs of S_6^{2+} are in agreement with those calculated earlier for $C_6H_6^{4-}$, N_6^{4-} , P_6^{4-} , S_6^{2+} , Te_6^{2+} , and $S_3N_3^-$ by: Li, J.; Liu, C.-W.; Lu, J.-X. *THEOCHEM* **1993**, 223.

can be compared. The related blue cyclic 7π radicals F_3 -CCSNSCCF₃ (in the gas phase)⁷⁴ and PhCNSNS (in CFCl₃)⁷⁵ have experimentally measured extinction coefficients of 40 (544 nm), 80 (780 nm), and ca. 20 (680 nm), respectively. Our assignment is also in agreement with the experimental magnetic circular dichroism²⁹ of a solution obtained by the oxidation of elemental sulfur with 30% oleum (four weeks reaction time). This showed that the blue species causing the band at 585 nm is highly symmetric, consistent with the D_{3d} symmetric S_6^{2+} dication rather than the asymmetric S_5^+ . However, the latter species also forms from S_8^{2+} in oleum solution as part of eq 16 that provides both, S_6^{2+} and S_5^+ ($K = 0.4$ in oleum, using $\Delta G = -RT \ln(K)$ and $\Delta G(\text{eq 16}) = +2$ kJ/mol in oleum), and was therefore detected by esr spectroscopy. The presence of S_5^+ in blue solutions likely may have misled previous workers to assume, according to our calculations wrongly, that only S_5^+ was the species giving rise to the blue color.

Oxidation of Sulfur by AsF₅ in the Presence of Facilitating Agent. The course of reaction of sulfur and AsF₅ is dramatically changed on addition of a facilitating agent, e.g., Br₂. Oxidation of sulfur does not stop with formation of S_8^{2+} (and its dissociation products in solution) but rapidly proceeds with formation of S_4^{2+} in the presence of a facilitator.^{17,18a-c,21} The facilitator lowers the energy barrier to the further oxidation of S_5^+ and of disproportionation reactions of $S_6^{2+}(\text{SO}_2)$ (reactions 11–13 in Table 1) leading to products that include S_4^{2+} . The computations suggest that the new radical cation S_4^+ may be present and detectable in sulfur dioxide solutions given on reaction of sulfur oxidized AsF₅ in the presence of a facilitating agent.

Why Solid $S_6(\text{AsF}_6)_2$ Has Not Been Prepared. Attempts to prepare solid $S_6(\text{AsF}_6)_2$ gave mixtures of $S_8(\text{AsF}_6)_2$ and $S_4(\text{AsF}_6)_2(X)$ ($X = \text{SO}_2$ or AsF_3 depending on the solvent).^{19,21,22} The enthalpy of the observed disproportionation of solid $S_6(\text{AsF}_6)_2$ in eq 23 was estimated from the Born–Fajans–Haber cycle shown in Figure 10.^{76,77}



$$\Delta H_r(\text{eq 23, s}) = -6 \text{ kJ/mol (using eq 11 theor in Table 1)}$$

$$\Delta H_r(\text{eq 23, s}) = -17 \text{ kJ/mol (using eq 11 expt in Table 1)}$$

The gas phase disproportionation enthalpy in the cycle in Figure 10 is essentially zero; however, the change in lattice energies slightly favors the solid state disproportionation in eq 23 by 6–17 kJ/mol. The small entropy of the disproportionation⁷⁸ additionally favors the right-hand side. The disproportionation may also be driven by the formation of a

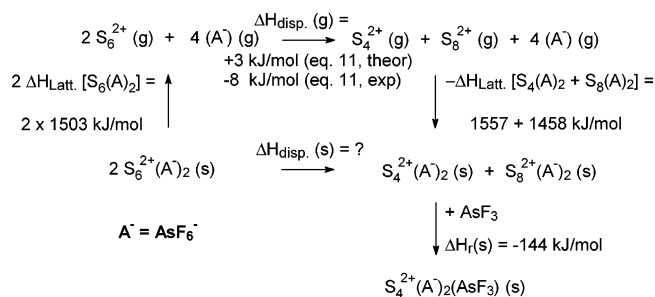
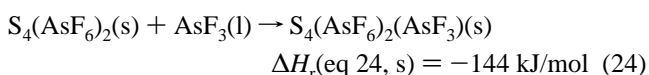


Figure 10. Born–Fajans–Haber cycle to estimate the disproportionation enthalpy ΔH_{disp} according to eq 23.

solvate $S_4(\text{AsF}_6)_2(\text{solvate})(s)$ precipitating from solution rather than $S_6(\text{AsF}_6)_2(s)$. No solvent free $S_4(\text{AsF}_6)_2(s)$ could be obtained from AsF₃ and SO₂, respectively, and $S_4(\text{AsF}_6)_2(\text{AsF}_3)(s)$ ¹⁹ or $S_4(\text{AsF}_6)_2(\text{SO}_2)(s)$,¹⁹ $S_4(\text{AsF}_6)_2(\text{SO}_2)_4(s)$ ⁷⁹ precipitated instead (X-ray). The enthalpy of reaction 24 was estimated as being exothermic by 144 kJ/mol.¹⁹



Therefore, the observed solid state disproportionation according to eq 23 may be drawn to the right-hand side by the inclusion of solvated AsF₃ or SO₂ molecules, and/or by the precipitation of insoluble $S_4(\text{AsF}_6)_2(X)$ ($X = \text{SO}_2$ or AsF_3). We note that $S_4(\text{AsF}_6)_2\text{AsF}_3$ was even obtained^{18d,19,20} from the reaction of sulfur and excess AsF₅ in anhydrous HF solvent according to 25.



Conclusion

Previous experimental and theoretical studies^{7,11,12,22} established that S_8^{2+} dissociated in very strong protonic acids and in SO₂ solution to give blue solutions containing the radical cation S_5^+ and by implication an unidentified species. In this work, we calculated the gas phase energetics of S_8^{2+} and its dissociation products and solvation energies in SO₂ and HSO₃F. These studies imply that in these solvents S_8^{2+} at low concentration largely dissociates to S_5^+ and $1/2S_6^{2+}$. The blue colors of such solutions have been attributed to S_5^+ ,^{7,12} however, by a comparison of published experimental UV–vis spectra with the computed spectra of S_n^+ ($n = 2–7$) and S_n^{2+} ($n = 3, 4, 6, 8$), we propose that the blue color likely largely arises from the $\pi^*-\pi^*$ transition of the previously unknown 10π S_6^{2+} dication. It is reasonable to assume that the blue color previously claimed to be S_5^+ in various acidic solvents is mostly due to S_6^{2+} .⁸⁰ The computations and a reinterpretation of the experimental data suggest that oxidation of elemental sulfur by AsF₅ in SO₂ ($S_{10}^{2+} \rightarrow S_4^{2+}$ region) gives $S_8^{2+}(\text{SO}_2)$, $S_6^{2+}(\text{SO}_2)$, $S_5^+(\text{SO}_2)$, and S_7^+ .

(79) Steden, F.; Beck, J.; Passmore, J. Unpublished results.

(80) Preliminary results showed a solution of $S_8(\text{AsF}_6)_2$ in a SO₂/SO₂ClF mixture to be red, and the UV–vis spectrum showed absorptions at 450 nm (shoulder, possibly S_7^+) and 710 nm (weak, possibly S_5^+) but no band at 585 nm. An ESR spectrum of the same sample showed the presence of S_5^+ and S_7^+ , strongly supporting the conclusion of the theoretical studies above that the blue color is due to S_6^{2+} and not to S_5^+ .¹⁶

(74) Brownridge, S.; Haddon, R. C.; Oberhammer, H.; Parsons, S.; Passmore, J.; Schriver, M. J.; Sutcliffe, L.; Westwood, N. P. C. *J. Chem. Soc., Dalton Trans.* **2000**, 3365.

(75) Passmore, J.; Sun, X. *Inorg. Chem.* **1996**, *35*, 1313.

(76) The lattice potential enthalpies were approximated by Jenkins' and Passmore's volume based equation⁷⁷ using the experimental thermochemical volumes $V_{\text{therm}}(\text{AsF}_6^-) = 110 \text{ \AA}^3$, $V_{\text{therm}}(S_4^{2+}) = 84 \text{ \AA}^3$, $V_{\text{therm}}(S_8^{2+}) = 174 \text{ \AA}^3$; that of S_6^{2+} was estimated as $(V(S_4^{2+}) + V(S_8^{2+}))/2$ giving $V_{\text{therm}}(S_6^{2+}) = 129 \text{ \AA}^3$.

(77) Jenkins, H. D. B.; Roobottom, H. K.; Passmore, J.; Glasser, L. *Inorg. Chem.* **1999**, *38*, 3609.

(78) Jenkins, H. D. B.; Glasser, L. To be published.

(SO_2) (no facilitating agent), and with a trace of facilitating agent also in addition gives $S_4^{2+}(SO_2)$ as well as the previously unknown $S_4^+(SO_2)$. The approximate relative concentrations of the sulfur radical cations in SO_2 solution observed by ESR^{7,12,17} are consistent with calculated ratios. These studies prompted us to re-examine the problem experimentally by esr studies, solution Raman spectroscopy, as well as solution magnetic measurements (Evans method) which will be the subject of future publications. However, preliminary results of solution magnetic measurements with the Evans method showed the presence of very large amounts of radicals present in SO_2 solutions of dissolved $S_8(AsF_6)_2$,⁸¹ and low-temperature esr studies also showed the presence of another radical ($S_4^{+?}$)¹⁷ in addition to S_5^+ and S_7^+ .

We note that the quality of computational results of this complexity can be predictive and not just a post experimental rationalization. Also, the calculations of the solvation energies of the sulfur cations by both the SCIPCM and COSMO methods are in good agreement, implying that solvation

energies of related species in other nonaqueous solvents that are not easily determined experimentally are now accessible by these computational methods.

Acknowledgment. We thank the Natural Sciences and Engineering Research Council NSERC of Canada (J.P., I.K.), and the Alexander von Humboldt Foundation in Bonn, Germany, for providing a Feodor-Lynen Fellowship (I.K.) and a Visiting Research Fellowship (J.P.). Acknowledgment is also made to the donors of the Petroleum Research Fund, administered by the American Chemical Society, for partial support of this research. Dr. Friedrich Grein (UNB) is thanked for very helpful discussions, as are Dr. Hong Bin Du for carefully checking the computed reaction energies and unpublished results, and Dr. Carsten Knapp for help with the manuscript.

Supporting Information Available: Discussion of the calculated sulfur cation geometries, the total energy of assessed species, calculation of zero point energies, stretching and bending mode scaling factors for S_6 , calculated vibrational spectra, additional other calculated dissociation reactions of the S_n^{2+} ($n = 4, 6, 8, 10$) dications, the extrapolated UV-vis spectrum of S_8^{2+} , and the solvation free energies of selected cations obtained by COSMO at the B3PW91/6-311+G* level. This material is available free of charge via the Internet at <http://pubs.acs.org>.

IC0207303

(81) Du, H. D.; Passmore, J. To be published.

(82) The difference between the theoretical and semiexperimentally derived enthalpies is due to the different calculated and experimental 1st ionization potential of S_6 . Photoionization studies of sulfur vapors show an appearance potential of S_6^+ of 868 kJ/mol⁶² while this property is calculated to be 834 kJ/mol [B3PW91/6-311+G(3df)//B3PW91/6-311+G*].

(83) Gillespie, R. J.; Passmore, J. *Acc. Chem. Res.* **1971**, *4*, 413 and references therein.